Time-Resolved Monitoring of Electrogenic Na^+-Ca^{2+} Exchange in the Isolated Cardiac Sarcolemma Vesicles by Using a Rapid-Response Fluorescent Probe†

David Baazov, Xiolan Wang, and Daniel Khananshvili*

The Department of Physiology and Pharmacology, Sackler School of Medicine, Tel-Aviv University, Tel-Aviv, Ramat-Aviv 69978, Israel

Received June 16, 1998; Revised Manuscript Received November 19, 1998

ABSTRACT: As a major Ca exit system in myocytes, the electrogenic Na^+-Ca^{2+} exchange is exposed to rapid changes of regulatory factors (e.g., cytosolic Ca) during the excitation−contraction coupling. The dynamic aspects of the exchanger response to regulatory factors have not been resolved in the past due to technical limitations. Here, we describe stopped-flow protocols for monitoring the electrogenic activity of Na^+-Ca^{2+} exchange in cardiac sarcolemma vesicles by using a rapid-response voltage-sensitive dye Merocyanine-540 (M540). The M540 signal of Na_o-dependent Ca efflux is generated by mixing the Ca-loaded vesicles with Na buffer, yielding 160 mM extravesicular Na and 6 μM Ca_{free}. This signal is inhibited by a cyclic peptide blocker (FRCRCFa), by a Ca ionophore (ionomycin), or by an electrogenic uncoupler (valinomycin or FCCP). The M540 signal of Na_o-dependent Ca efflux shows a rapid pre-steady-state burst (210 s^{-1}), followed by slow steady-state phase ($\leq$5 s^{-1}). Extravesicular (cytosolic) Ni inhibits both phases with an IC_{50} of 0.80 $\pm$ 0.24 mM. At an extravesicular pH of 6.0, the Na_o-dependent Ca efflux is able to generate the M540 signal, thereby supporting the idea that the stoichiometry of Na^+-Ca^{2+} exchange is not altered at low pH [Khanashvili, D., et al. (1995) *Biochemistry 34*, 10290−10297]. The M540 signal of Na_o-dependent Ca efflux is lost when the extravesicular Ca_{free} concentration drops to 0.2 μM. This effect cannot be explained by a lack of Ca access to extravesicular (cytosolic) transport sites, because the reaction of Na_o-dependent Ca efflux utilizes intravesicular Ca as a substrate. These data suggest that in sarcolemma vesicles a regulatory cytosolic Ca site controls the exchanger activity. The properties of this putative regulatory site do not resemble the properties of the "slow" Ca regulatory mode, observed in electrophysiological studies. Under saturating ionic conditions, the Na_o-dependent Ca efflux generates the initial rates of 21 mV/ms in the vesicles with a diameter of 3000−5000 Å. If a site density of 300−400 exchangers/μm^2 and a vesicular surface of 0.5 μm^2 are assumed, each vesicle may contain 150−200 exchanger molecules with a maximal turnover rate of 4000−5000 s^{-1}. This upper limit for turnover (no matter what the site density is) may put considerable restrictions on the exchanger capacity to mediate Ca entry in the cell under physiologically related conditions.

In myocytes, the cell membrane (sarcolemma) transporter NCX1 (*1*) catalyzes an electrogenic Na^+-Ca^{2+} exchange ($3Na^+$:Ca^{2+}) (*2*) which controls cytosolic Ca extrusion and muscle relaxation (*3*−*5*). Although this system has a potential to mediate Ca entry into the cell, a physiological relevance of this "reverse" mode is still not resolved (*6*−*9*). The Na^+-Ca^{2+} exchange cycle can be described as separate movements of Na and Ca ions through the exchanger (*10*−*14*). The rate-limiting and electrogenic mechanisms of partial reactions are still poorly understood (*15*−*22*). As an important protein, NCX1 is modulated by a number of cellular factors, but their molecular and kinetic mechanisms are still not known (for a review, see ref *18*).

Site-directed mutagenesis has identified functionally important amino acids and domains (*23*), but the understanding of structure−activity relationships clearly demands an application of more sophisticated analytical approaches. Fast perturbation techniques, such as the caged Ca release (*15*, *19*), voltage-jump (*13*, *14*), and stopped-flow (*24*) methods, have been recently introduced to achieve better time resolution. The Ca-jump experiments suggested that a net negative charge movement is associated with rapid Ca translocation (*15*, *19*), while the inward Na movement is 2−4 times slower than the outward Ca movement (*15*). This claim cannot easily explain the voltage-sensitive properties of steady-state Na^+-Ca^{2+} exchange and its partial reactions (for a review, see ref *18*). An alternative claim is that the rate-limiting translocation of positive charge is associated with Na transport involving the $(E{\cdot}Na_3)^+$ species (*11*, *16*, *21*, *25*, *27*). There is a growing body of evidence showing that the ion transport cycle of Na^+-Ca^{2+} exchange cannot be described by a simple consecutive mechanism, suggesting that multiple species (with undefined dynamic properties) may control the rate-limiting and voltage-sensitive properties (*15*−*18*, *21*, *25*, *27*, *28*).

NCX1 is strongly modulated by cytosolic protons (for a review, see ref *18*). These modulatory effects may function under certain pathophysiological conditions (e.g., acidosis or ischemia), in which the intracellular pH drops and the cytosolic Ca concentration rises. Patch-clamp experiments

† This work was partially supported by the U.S.A.-Israel Binational Foundation (BSF) and the Slezak Foundation.

* To whom correspondence should be addressed. Telephone: 972-3-640-9961. Fax: 972-3-640-9133. E-mail: dhanan@post.tau.ac.il.

10.1021/bi981429u CCC: $18.00
Published on Web 01/15/1999

in giant cardiac patches show that NCX1 is regulated by cytosolic Ca (*16*, *17*). This regulatory mode modifies the stationary levels of exchange currents within seconds, while Ca interacts with a cytosolic regulatory site that differs from the transport site (*16*, *17*). It is not clear how this slow Ca regulatory mode can control Na^+-Ca^{2+} exchange within a time scale of single and/or multiple cycles of action potential. Here, we show that in sarcolemma vesicles the activity of Na_o-dependent Ca efflux depends on extravesicular (cytosolic) Ca. Although this finding is consistent with the Ca-dependent regulation of the exchanger, the millisecond response kinetics of the putative Ca regulatory site does not seem to resemble the properties of slow Ca-dependent regulation, described previously by using the patch-clamp techniques.

The relative rates of partial reactions and the response of Na^+-Ca^{2+} exchange to voltage can be varied by modulatory factors (*18*, *21*, *25*, *27*). For example, at pH 6.0, the Na^+-Ca^{2+} exchange rates become "insensitive" to voltage change from −80 to 130 mV, while at pH 7.4, the exchange rate increases 6−7-fold in the same range of voltages (*21*, *27*). In addition, the ratio of Na^+-Ca^{2+}:$Ca^{2+}-Ca^{2+}$ exchange is reduced from 2.5 to 1.0, when the pH drops from 7.4 to 6.0 (*21*, *25*, *27*). Proton-dependent loss of voltage sensitivity and modification of exchange ratios can be explained by switching the rate-limiting step (e.g., electroneutral Ca transport may become rate-limiting instead of electrogenic Na^+ transport). However, previous studies could not exclude a possible modification of exchange stoichiometry by protons. Here, we show that the exchanger can generate a membrane potential at low pH, indicating that the electrogenic stoichiometry is not modified by protons.

The voltage-sensitive oxanol dyes have been used for monitoring the electrogenic activity of ion pumps (*29*−*31*). Unfortunately, these "slow-response" dyes cannot be utilized for millisecond monitoring of "rapid" transport processes. Here, we describe stopped-flow protocols for detecting the electrogenic Na^+-Ca^{2+} exchange in the preparation of isolated sarcolemma vesicles. A voltage-sensitive dye, Merocyanine-540 (M540[1]), has been chosen because it has a microsecond response (*32*, *33*). In myocytes, the sarcolemma membrane can exhibit large ion currents. However, the analysis of IV relationships, ion selectivity, and channel blockers provide no evidence for specific ion channel activities in isolated sarcolemma vesicles (*36*, *37*). In contrast, the ion flux capacities of Na^+-Ca^{2+} exchange are similar in the vesicular and cellular preparations (for a review, see ref *18*). Various biochemical tests show that the inside-out vesicles contribute to most Na^+-Ca^{2+} exchange activity in the preparation of sarcolemma vesicles (*21*, *26*, *34*, *38*, *39*). Thus, in stopped-flow experiments, the extravesicular (cytosolic) side of sarcolemma vesicles is exposed to added solutions.

[1] Abbreviations: Mops, 3-(*N*-morpholino)propanesulfonic acid; Tris, tris(hydroxymethyl)aminomethane; PMSF, phenylmethanesulfonyl fluoride; Oxanol-V, bis(3-phenyl-5-oxoisoxazol-4-yl)pentamethine oxanol; M540, [[3-sulfopropyl-2(3*H*)-benzoxazolylidene]-2-butenylidene]-1,3-dibutyl-2-thiobarbituric acid; EGTA, ethylene glycol bis(*β*-aminoethyl ether)-*N*,*N*,*N*′,*N*′-tetraacetic acid; BAPTA, 1,2-bis(2-aminophenoxyl)-ethane-*N*,*N*,*N*′,*N*′-tetraacetic acid; FCCP, carbonyl cyanide *p*-trifluoromethoxyphenylhydrazone; FRCRCFa, Phe-Arg-Cys-Arg-Cys-Phe-$CONH_2$; SLV, sarcolemmal membrane vesicles.

MATERIALS AND METHODS

The preparations of isolated cardiac sarcolemma vesicles (SLV) were obtained from fresh calf hearts in the presence of DNase and protease inhibitors as described previously (*21*−*26*). The vesicles can be stored at −70 °C for 3−4 months without any detectable loss of Na^+-Ca^{2+} exchange activity. The Na_i-dependent ^{45}Ca uptake was measured by semi-rapid-mixing quench as described previously (*21*−*23*, *25*−*27*, *40*). The SFM-3 stopped-flow system (BioLogic, Grenoble, France) was equipped with a thermostated three-syringe, two-mixer device, a MOS-200 optical system (mercury−xenon lamp, monochromator with fiber optics, and a high-voltage supplier), and a Hamamatsu R-376 photomultiplier. The syringe movements and the stop are electronically controlled and synchronized by a hardware microprocessor controller (each syringe is driven independently by an individual stepper motor). Equal volumes (30−40 μL) from syringe A and B were mixed at 37 °C by using the two-syringe mode. Prior to the stopped-flow experiments, Ca-loaded vesicles were obtained by incubating the SLV with 0.25−1.0 mM $CaCl_2$ and 0−10 mM KCl in MTS buffer [20 mM Mops/Tris (pH 7.4) and 0.25 M sucrose] for 14−18 h at 4 °C. The Ca-loaded vesicles (3−5 mg of protein/mL) were warmed to room temperature (22−25 °C) for 10−15 min and then thoroughly mixed with 1 μM valinomycin. Preparations not treated with valinomycin contained the same final concentration of ethanol (<0.5%). Before the Ca-loaded vesicles were placed in syringe A, they were preincubated with 1 μM M540 at 22−25 °C for 10−15 min. Unless indicated, syringe B contains MTBN buffer [20 mM Mops/Tris (pH 7.4), 0.16−1.6 mM BAPTA, 320 mM NaCl, and 0−10 mM KCl] with 1 μM M540. Nonspecific signals of M540 were estimated by clamping the membrane potential to "0 mV" by using the valinomycin-treated vesicles ($[K]_o = [K]_i$) or choline chloride (instead of NaCl) in syringe B. The Na_o-dependent Ca efflux was monitored with extravesicular fluo-3 (*24*) by mixing the Ca-loaded vesicles with MTBN buffer containing 10 μM fluo-3 and 0.3 mM BAPTA. Nonspecific Ca efflux from the vesicles was measured with choline chloride or KCl. In all stopped-flow recordings, time zero represents the initiation of mixing, while the arrow indicates the stop. The IC_{50} (±SE) was calculated with four-parameter logistic equations, equipped with statistical and robust weighting (GraFit v3.0, Erithacus Software Ltd.). Free calcium concentrations were measured and calculated in buffers as described previously (*24*, *48*).

In stopped-flow experiments, M540 was excited at 570 nm (with a monochromator connected to the observation chamber via fiber optics) and emission was monitored at either >595 nm (LG-595-F, Corion) or >610 nm (GG-610, BioLogic). The excitation at 570 nm is highly beneficial because the mercury−xenon lamp (L2482, Hamamatsu) has a sharp and bright illumination in this wavelength range. Although the signal amplitudes obtained by the LG-595-F filter are 1.3−1.4 times higher compared to those obtained with the GG-610 filter, the observed kinetics are practically indistinguishable for both filters. Fluo-3 was excited at a λ_{ex} of 475, and emission was monitored at a λ_{em} of >495 nm (GG-495 long path filter). The stopped-flow conditions (mixing volume, duration, flow rate, dead time, etc.) were controlled by the MPF program and the kinetics of recorded

traces analyzed with the BioKin 0.14 program equipped with the Padé-Laplace and Simplex modules (BioLogic). A total of 2500−8000 time points were taken for recording each mixing. The stopped-flow signals were monitored with a TC-100/15 cuvette (40 μL volume with a 10 mm light path) by fixing a high-voltage power supplier at 750−950 V. The excitation and emission spectra were monitored with a conventional SLM8000 spectrofluorimeter.

The size of sarcolemma vesicles was measured with photon correlation spectroscopy (*41*, *42*). The Malvern 4700 system (Malvern Instruments, Wocestershire, U.K.) is equipped with a PCS-100 laser spectrometer, goniometer, temperature controller, photomultiplier supply units, pumped filter system, and stepper motor. The light source was an argon ion laser (scattering angle can be selected between 10° and 150°, while the selected angle can be read to a precision of 0.1°). The photomultiplier was coupled to the amplifier discriminator (Malvern K7032 automeasure system). Particle sizes were calibrated by using standard polystyrene latex beads (0.055−0.24 μm).

Calcium flame photometry standard, polystyrene latex beads, protease inhibitors (PMSF, pepstatin, leupeptin, and aprotenin), DNase I (type DN-25, bovine pancreas), valinomycin, and EGTA were from Sigma (St. Louis, MO). Ionomycin was from Calbiochem (San Diego, CA). The glass microfiber filters (GF/C Whatman) were from Tamar (Jerusalem, Israel). $^{45}CaCl_2$ was purchased from DuPont NEN (Boston, MA). Merocyanine-540, BAPTA, and the free calcium calibration kit were from Molecular Probes, Inc. (Eugene, OR). Fluo-3 was from Teflabs (Austin, TX).

RESULTS

Fluorescence Response of M540 to Artificial Diffusion Potentials in Sarcolemma Vesicles. The M540 probe, equilibrated with sarcolemma vesicles, elucidates the specific excitation and emission spectra (Figure 1A). Fluorescence emission of M540 enhances by clamping the intravesicular positive potential in the valinomycin-treated sarcolemma vesicles (Figure 1B). In standard stopped-flow experiments, the dye was excited at 570 nm, because in this wavelength range the mercury−xenon lamp has a bright illumination line and the fluorescence emission was detected at either a λ_{em} of >595 nm or a λ_{em} of >610 nm (for more details, see Materials and Methods).

Stopped-flow kinetics of M540 fluorescence enhancement was monitored by clamping the intravesicular positive diffusion potentials in sarcolemma vesicles. The valinomycin-treated K-loaded vesicles (1 mM KCl) were mixed (t = 12 ms) to yield 200 mM extravesicular K (Figure 2A, trace a). For recording a nonspecific fluorescence signal (zero potential), the valinomycin-treated K-loaded vesicles (1 mM KCl) were mixed with KCl/LiCl buffer, yielding 1 mM extravesicular KCl and 199 mM LiCl (Figure 2A, trace d). The nonspecific signal (zero potential) is about 4 times smaller compared to the M540 signal obtained at 140 mV (Figure 2A). FCCP at 5 μM (electrogenic proton uncoupler) collapses the membrane potential of 140 mV to zero in a time-dependent manner (Figure 2A, trace b). More dramatic breakdown of membrane potential is obtained by 10 μM FCCP (Figure 2A, trace c). For a quantitative assay of intravesicular positive potentials, the valinomycin-treated

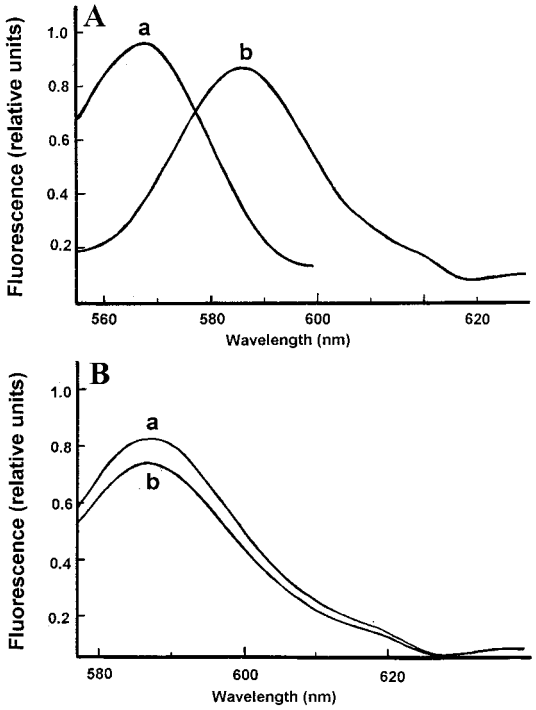

FIGURE 1: Fluorescence changes of M540 in response to diffusion potentials, clamped in sarcolemma vesicles. (A) The excitation (curve a) and emission (curve b) spectra of M540 were recorded by using a conventional spectrofluorimeter (SLM8000). The cuvette contained the MTK buffer [20 mM Mops/Tris (pH 7.4) and 160 mM KCl] with 1 μM M540 and sarcolemma vesicles (2 mg of protein/mL). Excitation spectra of 1 μM M540 were recorded with a λ_{em} of 610 nm (curve a). For monitoring the emission spectra, the dye was excited at a λ_{ex} of 540 nm (curve b). (B) Emission spectra of 1 μM M540 (λ_{ex} = 570 nm) were recorded in the KCl buffer (see above) containing the valinomycin-treated (curve a) or untreated (curve b) sarcolemma vesicles (1 mg of protein/mL).

vesicles (loaded with 1 mM K) were mixed to yield 1−350 mM extravesicular K (ionic conditions were balanced by Li). The nonspecific signal, obtained at zero potential, was subsequently subtracted from all recordings (Figure 2B). The voltage-sensitive signal of M540 increases exponentially with increasing diffusion potentials until the signal becomes saturated at 110−120 mV (Figure 2C). This is expected because the dye has a limited response capacity with respect to high voltages.

Optimization of Stopped-Flow Assay Conditions. To test a possible effect of M540 on the exchanger activity, the Na_i-dependent ^{45}Ca uptake was measured in sarcolemma vesicles in the presence and absence of 1 μM M540. Figure 3A shows that M540 has no significant effect on Na_i-dependent ^{45}Ca uptake. To avoid a time-consuming binding of M540 to membrane during the stopped-flow experiment, the vesicles were pre-equilibrated with 1 μM M540 first and then placed in syringe A (see Materials and Methods). M540 was also included in syringe B to avoid the dilution of the dye and its dissociation from the membrane during the stopped-flow experiment.

The signal size of Na_o-dependent Ca efflux is proportional to vesicular concentration, while large signals of M540 (1−3 V on output) can be routinely obtained with 1.5−2.3 mg of protein/mL of vesicles (not shown). The 40 μL cuvette with a 10 mm light path is most appropriate for stopped-flow monitoring of Na_o-dependent Ca efflux (the dead time is restricted to 8 ms with a maximal flow rate of 5 mL/s). The

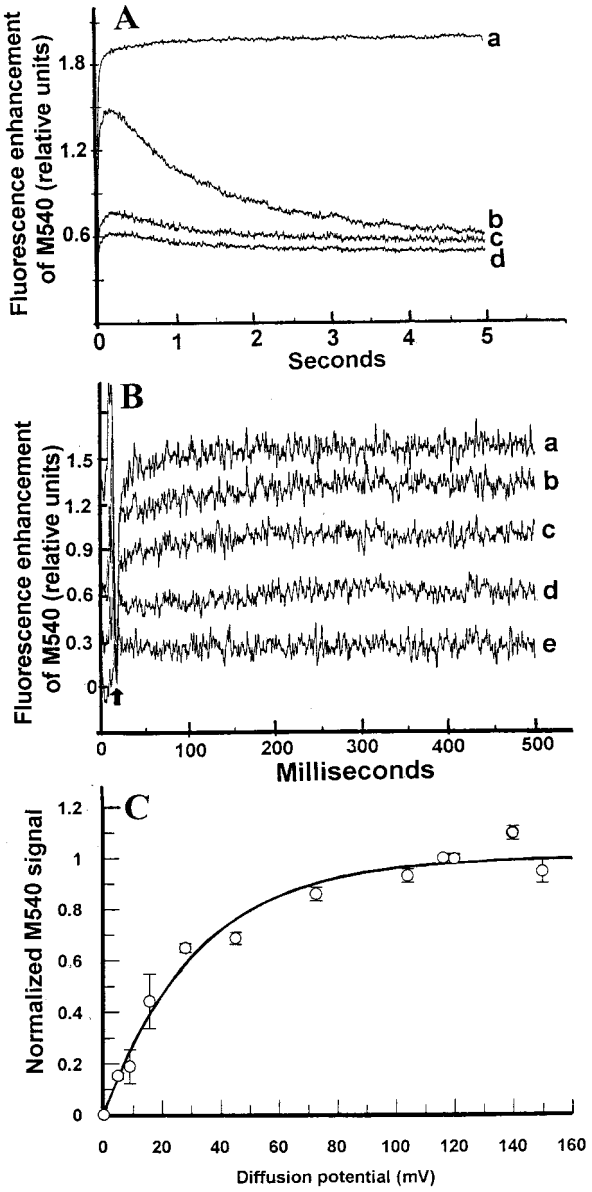

FIGURE 2: Stopped-flow recording of M540 signals in response to diffusion potentials, clamped in the sarcolemma vesicles. (A) Diffusion potentials were clamped by mixing (t = 12 ms) the valinomycin-treated K-loaded vesicles (1 mM KCl) with K-buffer [20 mM Mops/Tris (pH 7.4)] to give 200 mM KCl (traces a−c) or 1 mM KCl and 199 mM LiCl (trace d). The M540 signals were recorded in the absence of FCCP (traces a and d) or with 5 μM FCCP (trace b) or 10 μM FCCP (trace c) in both syringes. Traces a−d represent the average of six to eight recordings. (B) For calibrating the fluorescence changes of M540 in millivolts, the signals were monitored in the stopped-flow machine by using the valinomycin-treated vesicles. M540 was excited and monitored as described in Materials and Methods. The valinomycin-treated vesicles (preloaded with 1 mM KCl) were mixed with varying concentrations of K to give 116, 73, 45, 15, and 5 mV (curves a−e, respectively). The extravesicular ionic conditions were kept constant with LiCl. The nonspecific signals (zero potential) were recorded where $[K]_o = [K]_i = 1$ mM and subsequently subtracted from all recordings. Each trace represents the average of 15−17 mixings. (C) Normalized amplitudes of stopped-flow recordings, obtained at fixed $[K]_o/[K]_i$ ratios, were plotted vs calculated diffusion potentials. Membrane potentials were calculated with $\Delta\psi = 61.6 \text{ mV} \times \log([K]_o/[K]_i)$. Each point represents the mean ± SD of at least six recordings. The calculated line represents a single exponential for fitting the experimental points.

M540 amplitude of Na_o-dependent Ca efflux increases when the mixing time is increased from 8 to 12 ms (Figure 3B), suggesting that the kinetics of Ca buffering (by BAPTA,

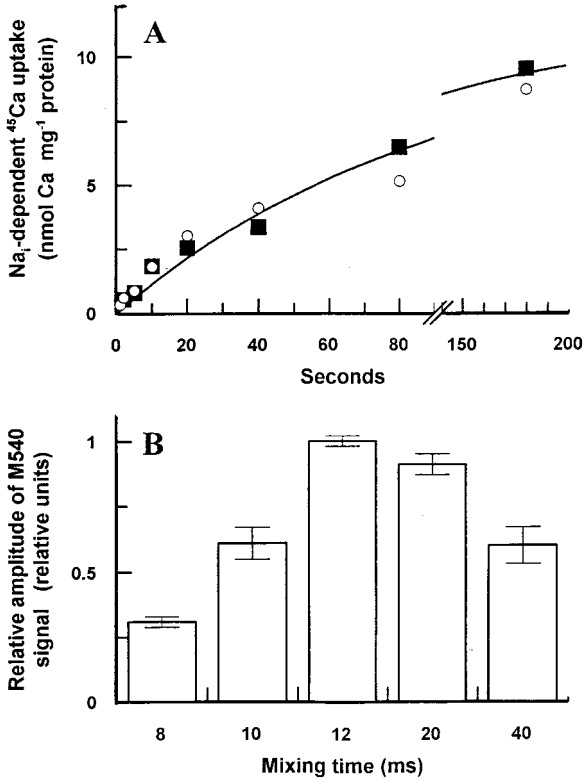

FIGURE 3: Optimal conditions for stopped-flow monitoring of Na_o-dependent Ca efflux by M540. (A) A possible inhibitory effect of M540 on the Na_i-dependent ^{45}Ca uptake was tested by using a preparation of isolated sarcolemma vesicles. Before the experiment, the cardiac sarcolemma vesicles (8 mg of protein/mL) were preloaded with 160 mM NaCl at 37 °C for 1 h. The Na-loaded vesicles were rapidly diluted (25-fold) in the MTS assay medium [20 mM Mops/Tris (pH 7.4) and 0.25 M sucrose] containing 37 μM $^{45}CaCl_2$ with (○) or without (■) 1 μM M540. The ^{45}Ca uptake was quenched by injecting the EGTA buffer in the semirapid mixer. The intravesicular ^{45}Ca level was measured by filtration on the GF/C filters as described in Materials and Methods. (B) The Ca-loaded vesicles (4−5 mg of protein/mL in MTS buffer equilibrated with 0.25 mM $CaCl_2$ and 1 mM KCl) were treated with or without valinomycin and before the experiment exposed to 1 μM M540 (see Materials and Methods). Stopped-flow mixings were carried out at the indicated mixing times. The Ca-loaded vesicles were mixed with NaCl/BAPTA buffer to give final concentrations of 160 mM NaCl, 0.125 mM BAPTA, 0.125 mM $CaCl_2$ (6 μM free Ca), 1 mM KCl, and 1 μM M540. The nonspecific signals were recorded at each mixing time by clamping the membrane potential to zero with valinomycin when $[K]_o = [K]_i = 1$ mM. Nonspecific signals were subtracted and normalized amplitudes plotted. Each column chart represents the mean ± SD, collected from 7−26 stopped-flow recordings.

membrane proteins, or lipids) and interaction of Ca with extravesicular site(s) may limit the exchanger activity. For example, a slow dissociation (79 s^{-1}) of Ca from BAPTA (*49*) may contribute to this. Truncated M540 signals of Na_o-dependent Ca efflux were obtained with prolonged (t > 12 ms) mixing times (Figure 3B), suggesting that M540 cannot register a certain fraction of membrane potential when the mixing time is too long.

M540 Signal of Electrogenic Na_o-Dependent Ca Efflux. The Na_o-dependent Ca efflux was initiated by mixing (t = 12 ms) the Ca-loaded vesicles (0.25 mM) with NaCl/BAPTA buffer (320 mM NaCl and 0.25 mM BAPTA) to give 160 mM extravesicular Na and ~6 μM Ca_{free}. The Na_o-dependent Ca efflux results in a rapid fluorescence enhancement of M540 (Figure 4A, trace a). The nonspecific fluorescence signal of Na_o-dependent Ca efflux was estimated by clamping

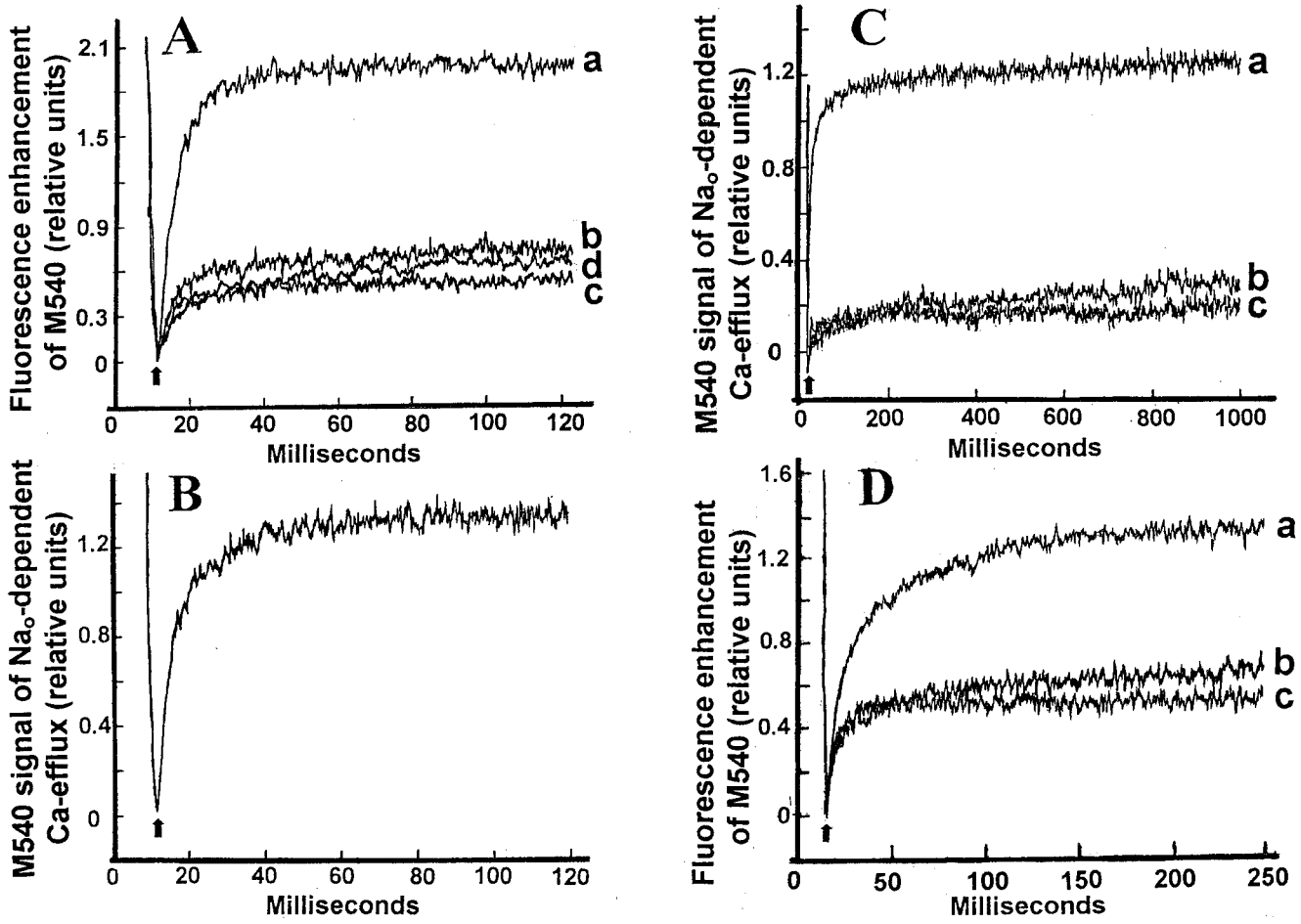

FIGURE 4: Stopped-flow monitoring of the M540 signal associated with electrogenic Na_o-dependent Ca efflux in the sarcolemma vesicles. (A) The Ca-loaded vesicles (4.3 mg of protein/mL in MTS buffer with 0.25 mM $CaCl_2$ and 1 mM KCl) were treated with or without valinomycin and then the vesicles incubated with 1 μM M540 before placing in syringe A. The 30 μL in syringe A was mixed ($t = 12$ ms) with 30 μL of MTBN buffer containing 1 mM KCl and 1 μM M540 (syringe B) to give final concentrations of 160 mM NaCl, 0.125 mM $CaCl_2$, and 0.125 mM BAPTA (trace a). For estimating the nonspecific M540 signals, the Ca-loaded vesicles were pretreated with 1 μM ionomycin (trace d) or the membrane potential was clamped to zero with 1 μM valinomycin when $[K]_o = [K]_i = 1$ mM (trace c). Alternatively, a nonspecific signal was recorded by substituting choline chloride for NaCl in syringe B (trace b). Other experimental conditions for stopped-flow monitoring of M540 fluorescence changes are described in Materials and Methods. Each trace represents the average of at least eight mixing experiments. (B) The membrane potential, generated by Na_o-dependent Ca efflux, was obtained by subtracting the "nonspecific" M540 signal (zero potential). The net M540 signal of Na_o-dependent Ca efflux was obtained by averaging the stopped-flow traces ($n = 24$), obtained in five independent experiments. (C) The membrane potential associated with Na_o-dependent Ca efflux was measured as described above in the absence (trace a) or presence of 200 μM FRCRCFa (trace b) or 2 mM Ca (trace c). Zero potentials were measured with the potassium/valinomycin system and subtracted from all traces as described above. Traces a−c represent the average of 10 stopped-flow recordings. (D) K-loaded (10 mM) vesicles were pre-equilibrated with the MTS buffer and mixed ($t = 12$ ms) with NaCl buffer and FRCRCFa in the presence (trace a) or absence (trace b) of Mg-ATP. Final concentrations of substances were 160 mM NaCl and 200 μM FRCRCFa with or without 4 mM Mg-ATP. The membrane potential was clamped to zero with 1 μM valinomycin when $[K]_o = [K]_i = 10$ mM (trace c). Traces a−c represent the average of seven or eight stopped-flow recordings.

a membrane potential to zero ($[K]_i = [K]_o = 1$ mM with valinomycin) (Figure 4A, trace c) or by substituting choline chloride for sodium (Figure 4A, trace b). Similar nonspecific signals were also obtained by substituting Li or K for Na (not shown). The mixing of ionomycin-treated Ca-loaded vesicles with NaCl/BAPTA buffer shows no voltage-sensitive signal of M540 (Figure 4A, trace d), meaning that the intravesicular Ca is obligatory for Na_o-dependent Ca efflux. A similar amplitude of the M540 signal was obtained with 0.25−5.0 mM intravesicular Ca (not shown), suggesting that these concentrations are saturating for Na_o-dependent Ca efflux. The M540 signal of reverse-mode Na^+-Ca^{2+} exchange (Na_i-dependent Ca influx) was tested by mixing the Na-loaded vesicles with 1 mM extravesicular Ca. No voltage-sensitive signal of M540 was obtained (not shown) in this case, because the dye does not sense the intravesicular negative potentials.

Figure 4B depicts a typical M540 signal of electogenic Na_o-dependent Ca efflux after subtracting the nonspecific signal. These recordings were reproducible for 18 different preparations of sarcolemma vesicles. The Na_o-dependent Ca efflux generates a rapid rise of M540 fluorescence, while 80−90% of the signal levels off within the first 70−100 ms (Figure 4B), followed by very slow increase of the rest signal (10−20%) up to 1000 ms (Figure 4C). The M540 signal of Na_o-dependent Ca efflux was validated by a cyclic peptide blocker (FRCRCFa) of the exchanger (*26*). FRCRCFa is a reasonably selective inhibitor of the exchanger which interacts from the cytosolic side (*27*, *34*, *35*). Figure 4C shows that 0.2 mM extravesicular FRCRCFa (trace b) or 2 mM Ca (trace c) inhibits about 90−95% of the M540 signal of Na_o-dependent Ca efflux. Similar FRCRCFa-dependent inhibition of Na_o-dependent Ca efflux was observed before by monitoring fluo-3 (*24*) or ^{45}Ca uptake (*26*). Thus, different

assay systems show that the inside-out vesicles contribute to most exchange activity. The functional "silence" of right-site-out vesicles is not clear, although they may be leaky (*39*).

The electrogenic activity of Na,K-ATPase was monitored in K-loaded vesicles in the presence of extravesicular Na and FRCRCFa to detect charge movements under conditions in which the Na^+-Ca^{2+} exchanger is completely inhibited. Figure 4D shows that the activation of the Na,K-ATPase by Mg-ATP generates the inside-positive potentials, which can be clamped to zero by potassium/valinomycin. These data show that the specific electrogenic activities of the exchanger and the Na,K pump can be separated in the same preparation of vesicles by using the same probe.

Comparing the Fluo-3 and M540 Signals of Na_o-Dependent Ca Efflux. The Na_o-dependent Ca efflux was monitored with the extravesicular Ca probe, fluo-3, or the voltage-sensitive probe M540 with a goal of evaluating a rapid saturation of M540 signals. In fluo-3 experiments, the Ca-loaded vesicles were mixed to give 160 mM extravesicular NaCl in the presence (trace a, Figure 5A) or absence (trace b, Figure 5A) of valinomycin ($[K]_o = [K]_i = 1$ mM). As can be expected for electrogenic Na_o-dependent Ca efflux monitored by fluo-3, potassium/valinomycin accelerates the rates of ion flux (traces a and b, Figure 5A). For monitoring the nonspecific Ca efflux, the Ca-loaded vesicles (loaded with 1 mM K) were mixed to give 160 mM extravesicular KCl in the presence (trace b, Figure 5B) or absence (trace c, Figure 5B) of valinomycin. The intravesicular positive potential (120 mV) has a very little (if any) effect on nonspecific Ca efflux (traces b and c, Figure 5B), providing no indication for significant acceleration of nonspecific "Ca leakage" by membrane potential. Moreover, for Ca-leaky vesicles one may expect to see a burst for "nonspecific Ca efflux", caused by rapid interaction of fluo-3 with Ca ($k_{on} = 7 \times 10^8$ M^{-1} s^{-1}, $k_{off} = 200-370$ s^{-1}). There is no indication of such a burst for nonspecific Ca efflux (trace c, Figure 5A), suggesting that the Ca-leaky vesicles dot not contribute to observed stopped-flow signals.

To compare the observed kinetics of M540 and fluo-3 signals, the Na_o-dependent Ca efflux was monitored under identical conditions. A comparison of M540 and fluo-3 signals of Na_o-dependent Ca efflux shows that the increases in intravesicular positive potentials do not arrest the exchanger activity at $t > 60$ ms, even though the M540 signal becomes nearly saturating at this stage (Figure 5C). These data suggest that the "saturating" signals of M540 represent a limited capacity of the dye to respond to high membrane potentials rather than a quasi-stationary state in which no net charge moves across the membrane.

Effect of Extravesicular Ni on the M540 Signal of Na_o-Dependent Ca Efflux. The effect of extravesicular (cytosolic) Ni on the electrogenic activity of Na^+-Ca^{2+} exchange was examined by monitoring the stopped-flow signal of M540 for up to 5 s. In these experiments, the Ca-loaded vesicles were mixed ($t = 12$ ms) with NaCl/BAPTA in the absence (Figure 6A, trace a) or presence of 0.5−5 mM Ni (Figure 6A, traces b−g). To show a net effect of extravesicular Ni on Na_o-dependent Ca efflux, the nonspecific fluorescence was recorded at zero potential (Figure 6A, trace h) and subsequently subtracted from all traces (Figure 6B, traces a−g). Increasing concentrations of extravesicular Ni inhibit

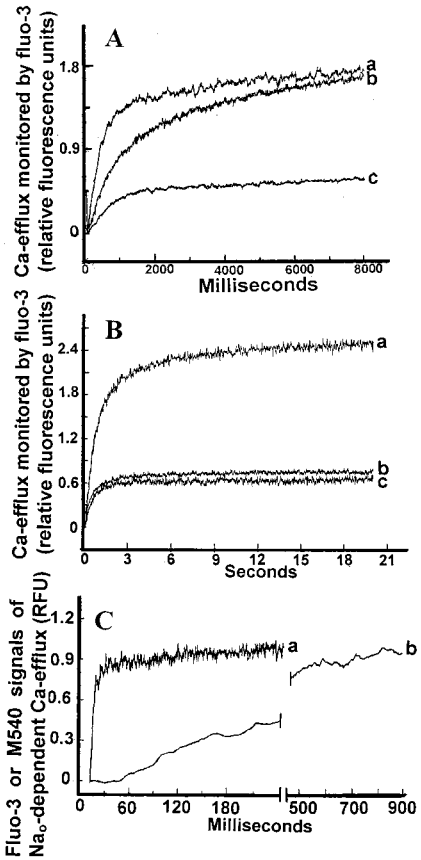

FIGURE 5: Comparing the fluo-3 and M540 signals for probing the Na_o-dependent Ca efflux in the sarcolemma vesicles. (A) The Na_o-dependent Ca efflux was detected by monitoring the extravesicular free calcium with fluo-3. The Ca-loaded vesicles (0.25 mM $CaCl_2$ and 1 mM KCl) in the MTS buffer were obtained as described in the legend of Figure 4. The Na_o-dependent Ca efflux was initiated by mixing the valinomycin-treated (trace a) or untreated (trace b) vesicles with MTBN/fluo-3 buffer. Equal volumes (30 μL) from syringe A (3 mg of protein/mL of Ca-loaded vesicles with 0.25 mM $CaCl_2$ and 1 mM KCl in MTS buffer) and syringe B (320 mM NaCl, 1 mM KCl, 0.3 mM BAPTA, and 10 μM fluo-3) were mixed. Nonspecific Ca efflux was monitored with 160 mM choline chloride instead of Na (trace c). Each trace represents the average of seven mixing experiments. (B) Nonspecific Ca efflux was monitored with 5 μM extravesicular fluo-3 by mixing equal volumes of Ca-loaded vesicles (0.25 mM Ca and 1 mM K in MTS buffer) and K-buffer (320 mM KCl, 0.3 mM BAPTA, and 10 μM fluo-3) (traces b and c). Prior to the stopped-flow experiment, the Ca-loaded vesicles were pretreated with (trace b) or without valinomycin (trace c). In the control experiment, the Na_o-dependent Ca efflux was monitored with 160 mM extravesicular Na (trace a). Other experimental conditions were similar to those described for panel A. (C) The Na_o-dependent Ca efflux was generated by mixing the Ca-loaded vesicles with the NaCl/BAPTA buffer to give final concentrations of 0.125 mM Ca, 0.15 mM BAPTA, and 160 mM NaCl. The Na_o-dependent Ca efflux was separately monitored with either 1 μM M540 (trace a) or 5 μM fluo-3 (trace b). All other experimental conditions were similar to those described in the legend of Figure 4 and for panel A. Traces a and b represent the average of seven stopped-flow recordings.

the Na_o-dependent Ca efflux in a dose-dependent manner, showing biphasic kinetics (Figure 6A). A rapid burst of the M540 signal reaches completion at 50 ms (Figure 6B), followed by a slow steady-state increase (Figure 6A). The saturating level of the M540 signal may reflect a limited sensitivity of the dye to respond to the increasing membrane potentials. Ni inhibits both the burst and slow phases with a similar IC_{50} of 0.80 ± 0.24 mM, suggesting that Ni may interact with the same inhibitory site (Figure 6C). Since Ni

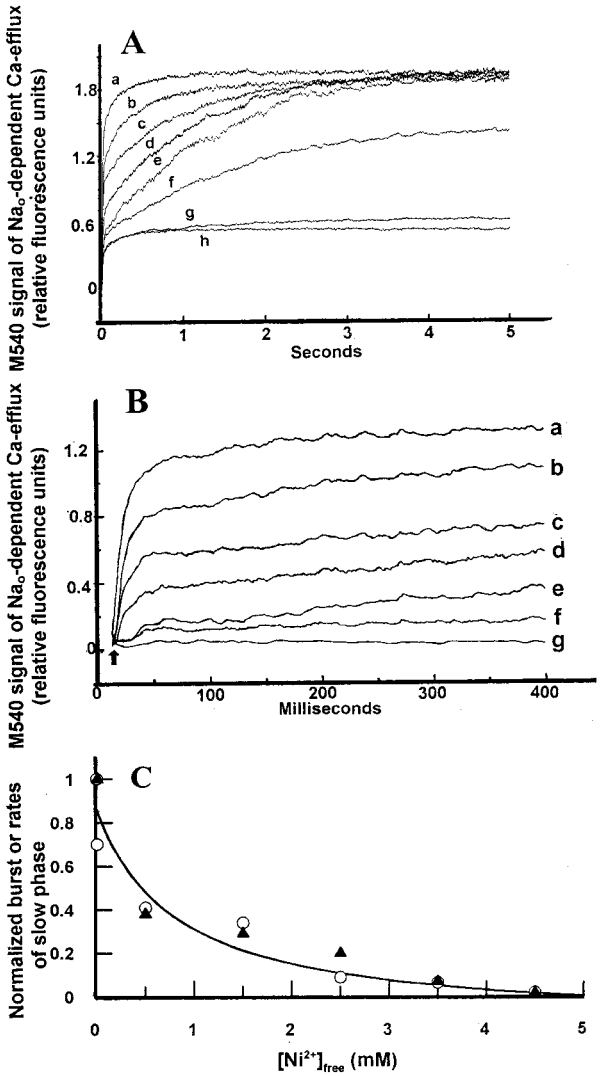

FIGURE 6: Effect of extravesicular (cytosolic) Ni^{2+} on the electrogenic Na_o-dependent Ca efflux. Before the experiment, the vesicles were loaded with 1 mM $CaCl_2$ (see Materials and Methods). (A) Syringe A contained the Ca-loaded vesicles (3 mg of protein/mL) in MTS buffer with 1 mM $CaCl_2$, 1 mM KCl, and 1 μM M540. Syringe B contained MTBN buffer with 1 μM M540, 1 mM KCl, and different concentrations of $NiCl_2$. The stopped-flow experiments were initiated by mixing the contents (30 μL) of syringe A and B (t = 12 ms) to give 0.5 mM BAPTA and varying concentrations of Ni: 0 (trace a), 0.5 (trace b), 1 (trace c), 2 (trace d), 3 (trace e), 4 (trace f), and 5 mM (trace g). The data were collected from three independent experiments, while each trace represents the average of 11−19 mixing experiments. Trace h represents zero potential, clamped by valinomycin. Other experimental conditions were similar to those described in the legend of Figure 4. (B) The first 400 ms of Na_o-dependent Ca efflux is pictured to show the effect of varying $[Ni]_{free}$ on the burst of the M540 signal. The nonspecific M540 signal (trace h in panel A) was subtracted from signals obtained at each concentration of Ni (traces a−g in panel A). *(C)* Nonspecific fluorescence signal of M540 (trace h in panel A) was subtracted from all traces, and normalized values of the burst at t = 50 ms (○) or the rates of the slow phase (▲) were plotted vs $[Ni]_{free}$. If a very high affinity ($K_d > 10^{-7}$ M) of BAPTA for Ni is assumed, the free concentrations of nickel can be calculated as $[Ni]_{free} = [Ni]_T - [BAPTA]_T$. The value of $IC_{50} \pm$ SE was calculated according to $Y/[1 + ([Ni]/IC_{50})]$, in which Y is the M540 signal in the absence of Ni. The line was computed to fit the experimental points, yielding an IC_{50} of 0.80 ± 0.24 mM.

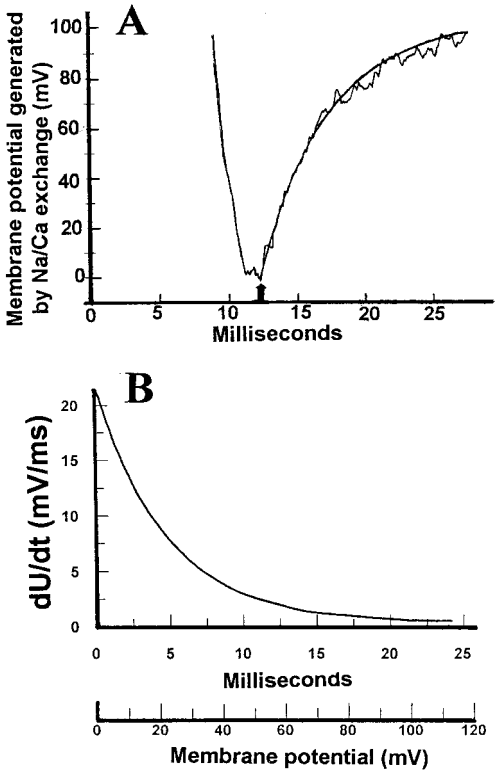

FIGURE 7: Quantitative estimation of initial rates of membrane potential generated by Na_o-dependent Ca efflux in sarcolemma vesicles. (A) The membrane potential generated by Na_o-dependent Ca efflux was measured under conditions described in the legends of Figures 4 and 6. The trace represents the average of 39 stopped-flow recordings. (B) The membrane potential generated by Na_o-dependent Ca efflux was converted into millivolts with the calibration curve depicted in Figure 2C. The solid line represents an optimal fit to the experimental data exhibiting the observed first-order rate constant of 210 s^{-1}. To demonstrate the dependence of dU/dt (the rates of generated membrane potentials) on time and voltage, the first derivative was taken from the fitted curve as shown in panel A.

binds to BAPTA more tightly than Ca, the BAPTA/Ca/Ni cocktail contains about 0.12 mM extravesicular Ca_{free} and 0.005−4.5 mM Ni_{free}. The control experiments show that in the absence of Ni, 0.1−0.2 mM extravesicular Ca_{free} inhibits 10−15% of the Na_o-dependent Ca efflux (not shown). Thus, the experimental limitations of metal buffering may not considerably alter the apparent affinity of Ni-dependent inhibition (Figure 6C). A possible competition between Ni and Ca for a common regulatory or transport site is a possibility which should be seriously considered in future experimental designs.

Initial Rates of Membrane Potential Generated by the Exchanger in the Vesicles. The M540 signals of Na_o-dependent Ca efflux were estimated in millivolts by using a calibration curve of fixed diffusion potentials (see Figure 2C). The reaction of Na_o-dependent Ca efflux arises from the intravesicular positive potentials with an apparent rate constant k_{app} of 210 ± 30 s^{-1} (Figure 7A), reaching a nearly saturating signal level at 100 mV. Taking the first derivative from the fitted curve (which proceeds via a time dependence of dU/dt) shows that the Na^+-Ca^{2+} exchange activity can generate the membrane potential (U) with the initial rate dU/dt of 21 mV/ms (Figure 7B). Moreover, as a result of the exchanger activity, the increase of intravesicular potentials by every 25 mV reduces the dU/dt rates ~2.5-fold. The slope of this IV relationship represents an upper limit that one may expect for a transport system which translocates a single net charge per cycle (*43*, *44*). More shallow IV curves were

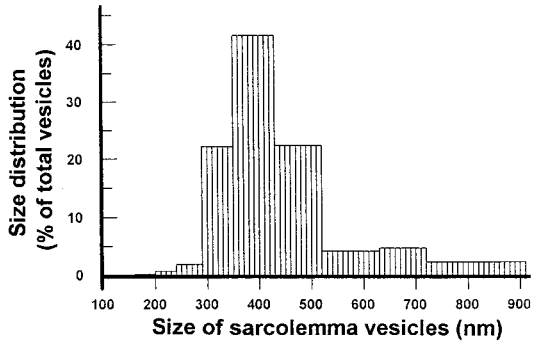

FIGURE 8: Particle size distribution in the preparation of isolated sarcolemma vesicles, measured by photon correlation spectroscopy. The size of isolated sarcolemma vesicles (50 μg of protein/mL) was measured in MTS buffer [20 mM Mops/Tris (pH 7.4) and 0.25 M sucrose] by using photon correlation spectroscopy. The light source was the argon ion laser (25 W, 488 nm). The scattering angle was adjusted to 90°. Other details are described in Materials and Methods.

observed previously by measuring the steady-state ion fluxes in vesicles or electric currents in excised and whole cell patches (for a review, see ref *18*).

A knowledge of vesicular size may provide complementary information about the rate and density of charge movements through the sarcolemma membrane (see Discussion). Therefore, the size distributions of isolated sarcolemma vesicles were measured by using the quasi-elastic light scattering technique (photon correlation spectroscopy). As can be observed from Figure 8, the vesicular size ranges from 200 to 900 nm, although more than 85% of the vesicles have a diameter of 300−500 nm. Although the profile of particle size distribution of sarcolemma vesicles was variable in four different preparations, it is a general observation that the average diameter of vesicles is approximately 400 nm. Thus, with a vesicular radius of 200 nm, the surface area ($A = 4\pi r^2$) of a single vesicle can be calculated as 0.5 μm^2.

Effect of Extravesicular (Cytosolic) Calcium or pH on the Electrogenic Na_o-Dependent Ca Efflux. The M540 signal of Na_o-dependent Ca efflux was monitored at an extravesicular pH of 6.0 with a goal of testing the ability of the exchanger to generate the membrane potential at acidic pH. The M540 signal of Na_o-dependent Ca efflux, obtained at pH 6.0 (Figure 9A, trace b), is comparable to the control experiment at pH 7.4 (Figure 9A, trace a). At both pHs, the signal is collapsed by clamping the membrane potential to zero with potassium/valinomycin (Figure 9A, traces c and d). Thus, at pH 6.0, the Na^+-Ca^{2+} exchanger retains its capacity for electrogenic stoichiometry of ion exchange. This conclusion supports a previous proposal suggesting that the protons can change the status of the rate-limiting pathway (and not the stoichiometry of ion exchange) in such a way that the "electroneutral" Ca transport step may become rate-limiting (*21*, *25*, *27*). This kind of rate-limiting switch of the electrogenic step may result in a "voltage-insensitive" Na^+-Ca^{2+} exchange, observed in the experiment (*21*, *25*).

In standard stopped-flow experiments, the Na_o-dependent Ca efflux is monitored with 160 mM extravesicular NaCl and 6−20 μM free calcium. To test a possible regulation of the exchanger activity by extravesicular (cytosolic) calcium, the M540 signal of Na_o-dependent Ca efflux was monitored in sarcolemma vesicles with 160 mM extravesicular NaCl and 0.2 μM free calcium. Figure 9B shows that the Na_o-dependent Ca efflux cannot generate the membrane potential with 0.2 μM extravesicular free Ca (trace b), while a normal M540 signal of Na_o-dependent Ca efflux is obtained with 6 μM extravesicular free Ca (trace a). This effect cannot be explained by a lack of Ca access to the extravesicular (cytosolic) transport site. This is because the extravesicular Ca is not obligatory by definition for the reaction of Na_o-dependent Ca efflux (in this mode, Ca must interact with intravesicular transport sites). Therefore, these data suggest that the putative cytosolic Ca site differs from the transport sites of the exchanger and is able to control the exchanger activity in the preparation of isolated sarcolemma vesicles. The properties of this putative regulatory site do not resemble those of the "slow" modulation described previously in electrophysiological experiments (*16*, *17*). Notably, the increase of extravesicular free Ca concentration from 6 to 50 μM causes a small increase of the M540 signal (not shown), suggesting that the putative regulatory site may have a high affinity for Ca. Further systematic studies are needed for characterizing the affinity and rate constants of the putative Ca regulatory site.

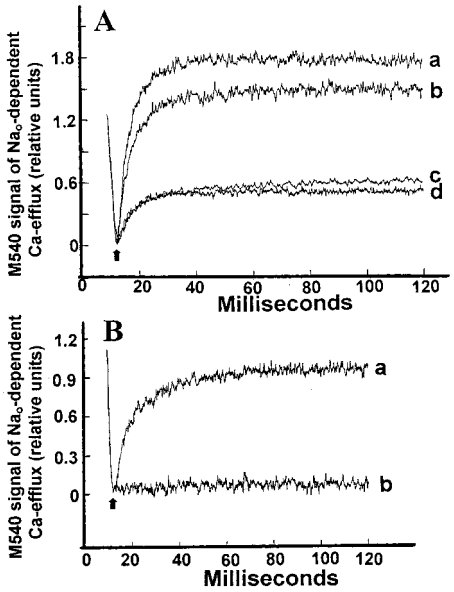

FIGURE 9: Effect of extravesicular (cytosolic) pH and calcium on the electrogenic activity of Na_o-dependent Ca efflux. (A) The M540 signal of Na_o-dependent Ca efflux was monitored by mixing (t = 12 ms) the Ca-loaded vesicles (3 mg of protein/mL) with NaCl/BAPTA, yielding an extravesicular pH of 6.0 or 7.4. The pH in syringe B was controlled by either 40 mM Mes/Tris (pH 5.3) or Mops/Tris (pH 7.4) to give a final extravesicular pH of 6.0 (trace b) or 7.4 (trace a). The membrane potential was clamped to zero by potassium/valinomycin at pH 7.4 (trace c) or 6.0 (trace d). Traces a−d represent the average of 12 recordings. (B) The membrane potential generated by Na_o-dependent Ca efflux was monitored with M540 with 6 (trace a) or 0.2 μM free Ca (trace b). Other experimental conditions were similar to those described for panel A and in the legend of Figure 4; otherwise, the MTBN buffer in syringe B contained either 0.25 (trace a) or 1.6 mM BAPTA (trace b). The data were collected from three independent experiments, while traces a and b are the average of 16−18 mixing experiments.

DISCUSSION

Stopped-Flow Monitoring of Electrogenic Na_o-Dependent Ca Efflux in Sarcolemma Vesicles. The clamping of artificial diffusion potentials in the sarcolemma vesicles results in specific fluorescence changes of M540 (Figure 1B). The

rapid kinetics of voltage-sensitive enhancement of M540 fluorescence can be monitored by stopped-flow techniques (Figure 2B). M540 has no detectable effect on the Na_i-dependent ^{45}Ca uptake (Figure 3A), suggesting that the dye itself does not have harmful effects on the exchanger activity under the experimental conditions tested. Electrogenic proton uncoupler FCCP collapses the diffusion potentials (clamped by potassium/valinomycin) in sarcolemma vesicles in a concentration- and time-dependent manner (Figure 2A). In valinomycin-treated vesicles, the amplitude of the M540 signal increases exponentially with increasing $[K]_o/[K]_i$ values until the dye becomes insensitive to intravesicular positive potentials at 110−120 mV (Figure 2C). These data show that the membrane potentials can be quantitatively measured by M540 in the preparation of sarcolemma vesicles, although the dye sensitivity is restricted at high intravesicular potentials.

In standard stopped-flow experiments, the Na_o-dependent Ca efflux is initiated by mixing ($t = 12$ ms) the Ca-loaded vesicles with Na/BAPTA to yield 160 mM extravesicular Na and 6−20 μM free Ca. The Na_o-dependent Ca efflux results in a rapid enhancement of M540 fluorescence (Figure 4A). The M540 signal of Na_o-dependent Ca efflux depends on the duration of the mixing time, showing an optimum at $t = 12$ ms (Figure 3B). This means that the kinetics of Ca buffering (by BAPTA, membrane lipids, and proteins) and a possible interaction of Ca with a putative extravesicular domain(s) may limit the exchanger activity in time. A signal truncation of Na_o-dependent Ca efflux with prolonged mixing times (Figure 3B) may represent technical restrictions for signal recording during the mixing.

The clamping of membrane potential to zero with potassium/valinomycin or substituting monovalent cations (choline chloride, potassium, or lithium) for extravesicular Na reduces the M540 signal dramatically (Figure 4A). The treatment of Ca-loaded vesicles with ionomycin results in a loss of the signal, suggesting that intravesicular Ca is obligatory for Na_o-dependent Ca efflux (Figure 4A). Moreover, the M540 signal of Na_o-dependent Ca efflux is effectively inhibited by a cyclic peptide blocker FRCRCFa (Figure 4C). All nonspecific signals (obtained with potassium/valinomycin, monovalent cations, ionomycin, FCCP, or FRCRCFa) have a similar amplitude, accounting for about 20−25% of the M540 signal associated with Na^+-Ca^{2+} exchange. Under conditions in which the Na^+-Ca^{2+} exchanger is completely inhibited by FRCRCFa, a rapid addition of Mg-ATP to K-loaded vesicles results in a fluorescence enhancement for M540 (Figure 4D). These data suggest that the electrogenic Na,K pump activity can be separated from the exchanger activity by using the same probe (M540) and preparation of vesicles.

Biphasic Kinetics of Electrogenic Na^+-Ca^{2+} Exchange and the Inhibitory Effect of Extravesicular Ni^{2+}. The mixing ($t = 12$ ms) of Ca-loaded vesicles with NaCl/BAPTA results in biphasic kinetics exhibiting a rapid fluorescence enhancement of M540 (80−90% of the signal increases at 210 s^{-1}), followed by a slow phase (10−20% of the signal increases at ≤ 5 s^{-1}) (Figure 4C). The observed rapid phase may stand for pre-steady-state kinetics, while the slow phase may represent a switch of the exchanger activity to steady-state kinetics. The rapid and slow phases were more clearly separated by detecting the extravesicular effect of Ni on the M540 signal of Na_o-dependent Ca efflux. Although the underlying mechanisms of biphasic kinetics are not clear at this moment, it would be reasonable to assume that the increase in intravesicular positive potentials slows the rates of exchanger-mediated charge movement into the vesicles (Figure 7B).

In the presence of varying concentrations of extravesicular Ni, the M540 signals show a rapid burst, followed by a slow (>50 ms) increase of the signal until the dye becomes insensitive to increasing membrane potentials (Figure 6A). Notably, the extravesicular Ni inhibits both the burst and slow phase rates with a very similar IC_{50} of 0.80 ± 0.24 mM (Figure 6A). These experiments provide the evidence that both the rapid and slow phases (even in the absence of Ni) belong to the electrogenic activity of Na^+-Ca^{2+} exchange. Although the interaction of Ni with two distinct (transport or regulatory) sites cannot be excluded at this moment, the present data support the idea that Ni may interact with the same putative site. An alternative possibility is that the biphasic inhibition of electrogenic Na^+-Ca^{2+} exchange represents the interaction of Ni with different transport and/or regulatory sites. For example, the burst amplitude may represent the interaction of Ni with the transport site, while the slow phase may reflect the Ni binding to the regulatory site. Further experimentation is needed for segregating these possibilities.

Initial Rates of Electrogenic Na^+-Ca^{2+} Exchange Activity. A specific surface area ($A = 4\pi r^2$) of a single vesicle contains a fixed number of exchanger molecules (n_E), which can generate the electric current I_E. The rate of charge (Q) translocation or current ($dQ/dt = I_E$) is proportional to dU/dt, by which it charges the membrane capacitor C_m (1 μF/cm^2), given as $dQ/dt = I_E = AC_m(dU/dt)$. With the experimentally measured initial rate dU/dt of 21 mV/ms (Figure 7A) and average vesicular surface A of 0.5 μm^2 (r_{ev} = 2000 Å) (Figure 8), one can determine that the cardiac Na^+-Ca^{2+} exchanger has a maximal capacity to translocate $\sim 1.1 \times 10^6$ charges s^{-1} μm^{-2}. Integration of the dU/dt data with time shows that ~3400 charges can be translocated in a single vesicle until the membrane potential reaches 100 mV (Figure 7B). The initial rate of 21 mV/ms represents a translocation of 600−700 charges/ms. This initial rate of charge translocations may represent three to seven turnovers, assuming that each single vesicle contains 150−200 exchanger molecules (see below).

The pre-steady-state turnover rate of the exchange cycle can be derived from the stopped-flow data if the particle size and site density are independently estimated. A fixed number of exchanger molecules (n_E) can generate the current I_E ($=n_E e_o k_o$), in which k_o is the rate constant (turnover number) of the exchange cycle and e_o is an elementary charge ($e_o = 1.6 \times 10^{-19}$ C). If Φ_E is the site density of active exchanger molecules in the sarcolemma membrane (n_E/A), the turnover number can be derived from $k_o = C_m(dU/dt)/\Phi_E e_o$. Independent studies with H^3-labeled antibodies suggest that in neonatal sarcolemma membranes the exchanger site density Φ_E is in the range of ≅800 copies/μm^2 (*45*), while the Φ_E value is reduced 2−3-fold in the adult sarcolemma membranes (*46*). Photon correlation spectroscopy measurements show that 90−95% of the vesicles have a diameter in the range of 3000−5000 Å (Figure 8), so with the r_{ev} of 2000 Å, the surface area of a single vesicle (A_{ev}) can be estimated as 0.5 μm^2. By combing the initial rate of

membrane potential ($dU/dt = 21$ mV/ms), the vesicular surface ($A_{ev} = 0.5\ \mu m^2$), and the exchanger site density in the sarcolemma membrane ($\Phi = 250-400$ copies/μm^2), one can conclude that each vesicle may contain 150−200 copies of active exchanger molecules exhibiting a maximal turnover rate k_o of 4000−5000 s^{-1}. This k_o value is derived under standard conditions (zero membrane potential and 37 °C) in which the exchanger works at saturating ionic concentrations at both sides of the membrane. A precaution has to be taken that the value of the turnover number could be revised if the site density of NCX1 is considerably different in the rat and calf sarcolemma membranes. Whatever the site density of NCX1 is, the upper limit of the turnover number may put considerable restrictions on exchanger-mediated Ca entry into the cell under physiologically related conditions (*18*, *47*).

Na^+-Ca^{2+} Exchange Is Able To Generate the Membrane Potential at Acidic Extravesicular pH. The cardiac sarcolemma Na^+-Ca^{2+} exchanger is strongly modulated by pH, presumably because protons may interact with both the transport and regulatory domains (*16*, *18*, *21*, *25*, *27*, *50*). In isolated sarcolemma vesicles, a decrease of extravesicular (cytosolic) pH from 7.4 to 6.1 results in a loss of the exchanger capacity to respond to varying voltages, while the same pH shift diminishes the Na^+-Ca^{2+}:$Ca^{2+}-Ca^{2+}$ exchange ratio from 2.5 to 1.0 (*21*, *25*, *27*). Two principle mechanisms may account for these data. In the first mechanism, the protons may modify the rate-limiting pathway in such a way that the voltage-insensitive step (e.g., Ca^{2+} transport) may become rate-limiting without altering the stoichiometry of $3Na^+$:Ca^{2+}. If this is correct, the exchanger must still be able to generate the membrane potential in the vesicles even at acidic extravesicular (cytosolic) pH. In an alternative mechanism, the protons may directly alter the stoichiometry of ion exchange, yielding an electroneutral (e.g., $2Na^+$:Ca^{2+} or $3Na^+$:Ca^{2+},H^+) mode of Na^+-Ca^{2+} exchange. In this case, the exchanger would not be able to generate the membrane potential. To distinguish between these two possibilities, the electrogenic activity of Na_o-dependent Ca efflux has been monitored at either pH 6.0 or 7.4. As can be seen from Figure 9A, the Na^+-Ca^{2+} exchanger is able to generate the membrane potential in sarcolemma vesicles even at low pH. These data are consistent with the idea that protons do not alter the electrogenic stoichiometry of Na^+-Ca^{2+} exchange, although protons can modify the rate-limiting status of the electrogenic step. Thus, as predicted before the proton-induced loss of the exchanger, as a response to voltage changes, represents a kinetic rather than a stoichiometric effect (*25*, *27*).

Inactivation of Na^+-Ca^{2+} Exchange by Rapid Decrease of Extravesicular (Cytosolic) Calcium. The Ca-dependent regulation of the exchanger activity never has been detected before in the preparation of isolated sarcolemma vesicles. It is not clear whether this failure is caused by disruption of functional properties of the exchanger in the preparation of isolated sarcolemma vesicles or technical limitations associated with radioactive ion flux where assay may not permit the detection of Ca-dependent regulation. For example, in the assay of Na_i-dependent ^{45}Ca uptake, the cytosolic side of sarcolemma vesicles is usually exposed to 10−20 μM ^{45}Ca, suggesting that a putative regulatory extravesicular (cytosolic) site might be occupied in this case. In a reverse mode (the Na_o-dependent ^{45}Ca efflux), the initial rates of ^{45}Ca efflux cannot be quantitatively assayed because of high ^{45}Ca background counts on the filter. To identify a putative Ca regulatory site in the preparation of isolated sarcolemma vesicles, the Na_o-dependent Ca efflux was monitored with M540 in the presence of 0.2 μM extravesicular free calcium. In contrast to the control experiment with 6 μM calcium, the exchanger cannot generate the membrane potential in the presence of 0.2 μM extravesicular free calcium (Figure 9B). These data cannot be explained by a lack of extravesicular Ca access to the transport site, because in the present experimental setup the extravesicular Ca is not obligatory for the reaction of Na_o-dependent Ca efflux. By definition, in this mode of Na^+-Ca^{2+} exchange, the extravesicular Na must interact with outwardly exposed transport sites of the exchanger, while the intravesicular Ca must interact with inwardly exposed transport sites. Therefore, these data show in the preparation of isolated sarcolemma vesicles the exchanger activity can be modulated by extravesicular (cytosolic) Ca. This Ca-dependent regulation of the exchanger in sarcolemma vesicles does not resemble the properties of a slow Ca-regulatory mode described previously in electrophysiological studies (*14*, *16*, *51*). More detailed kinetic analysis is necessary for separating the "rapid" and "slow" pathways of Ca-dependent regulation of the exchanger.

REFERENCES

1. Nicoll, D. A., Longoni, S., and Philipson, K. D. (1990) *Science 250*, 562−564.
2. Reeves, J. P., and Hale, C. C. (1984) *J. Biol. Chem. 259*, 7733−7739.
3. Bridge, J. H. B., Smolley, J. R., and Spitzer, K. W. (1990) *Science 248*, 376−378.
4. Bers, D. M. (1991) in *Excitation-Contraction Coupling and Cardiac Contractile Force*, pp 1−258, Kluwer Academic Press, Dordrecht, The Netherlands.
5. Nobel, D., Nobel, S. J., Bett, G. C. L., Earm, Y. E., Ho, W. K., and So, I. K. (1991) *Ann. N.Y. Acad. Sci. 639*, 334−354.
6. Leblanc, N., and Hume, J. R. (1990) *Science 248*, 372−375.
7. Levi, A. J., Brooksby, P., and Hancox, J. C. (1994) *Cardiovasc. Res. 27*, 1743−1757.
8. Cannel, M. B., Cheng, H., and Lederer, W. J. (1995) *Science 268*, 1045−1049.
9. Lopez-Lopez, J. R., Shacklock, P. S., Balke, C. W., and Wier, W. G. (1995) *Science 268*, 1042−1045.
10. Khananshvili, D. (1990) *Biochemistry 29*, 2437−2442.
11. Hilgemann, D. W., Nicoll, D. A., and Philipson, K. D. (1991) *Nature 352*, 715−718.
12. Hilgemann, D. W. (1991) *Ann. N.Y. Acad. Sci. 639*, 126−139.
13. Hilgemann, D. W. (1996) *Biophys. J. 71*, 759−768.
14. Hilgemann, D. W. (1996) *Ann. N.Y. Acad. Sci. 779*, 136−158.
15. Kappl, M., and Hartung, K. (1996) *Biophys. J. 71*, 2473−2485.
16. Matsuoka, S., and Hilgemann, D. W. (1992) *J. Gen. Physiol. 100*, 963−1001.
17. Matsuoka, S., and Hilgemann, D. W. (1994) *J. Physiol. 476*, 443−458.
18. Khananshvili, D. (1998) in *Ion Pumps-"Advances in Molecular and Cell Biology"*, Vol. 23B, pp 311−358, Life Sciences Program, JAI Press Inc., Middlesex, U.K.
19. Niggli, E., and Lederer, W. J. (1991) *Nature 349*, 621−624.
20. Khananshvili, D. (1991) *J. Biol. Chem. 266*, 13764−13769.
21. Khananshvili, D., and Weil-Maslansky, E. (1994) *Biochemistry 33*, 312−319.
22. Li, J., and Kimura, J. (1991) *Ann. N.Y. Acad. Sci. 639*, 48−60.
23. Nicoll, D. A., Hryshko, L. V., Matsuoka, S., Frank, J. S., and Philipson, K. D. (1996) *Ann. N.Y. Acad. Sci. 779*, 86−92.

24. Khananshvili, D., Baazov, D., Weil-Maslansky, E., Shaulov, G., and Mester, B. (1996) *Biochemistry 35*, 15933−15940.
25. Khananshvili, D., Weil-Maslansky, E., and Baazov, D. (1996) *Ann. N.Y. Acad. Sci. 779*, 217−236.
26. Khananshvili, D., Shaulov, G., Weil-Maslansky, E., and Baazov, D. (1995) *J. Biol. Chem. 270*, 16182−16188.
27. Khananshvili, D., Shaulov, G., and Weil-Maslansky, E. (1995) *Biochemistry 34*, 10290−10297.
28. Matsuoka, S., Philipson, K. D., and Hilgemann, D. W. (1996) *Ann. N.Y. Acad. Sci. 779*, 159−170.
29. Appel, H.-J., and Bersh, B. (1987) *Biochim. Biophys. Acta 903*, 480−494.
30. Goldshleger, R., Shahak, Y., and Karlish, S. J. D. (1990) *J. Membr. Biol. 113*, 139−154.
31. Clarke, R. J., Apell, H.-J., and Lauger, P. (1989) *Biophys. Chem. 34*, 225−237.
32. Verkman, A. S., and Frosch, M. P. (1985) *Biochemistry 24*, 7117−7122.
33. Verkman, A. S. (1987) *Biochemistry 26*, 4050−4056.
34. Khananshvili, D., Mester, B., Saltoun, M., Shaulov, G., and Baazov, D. (1997) *Mol. Pharmacol. 51*, 126−131.
35. Hobai, I. A., Khananshvili, D., and Levi, A. J. (1997) *Pflugers Arch. 433*, 455−463.
36. Van Alstyne, E., Burch, R. M., Knikelbein, R. G., Hungerford, R. T., Gower, E. J., Webb, J. G., Poe, S. L., and Lindenmayer, G. E. (1980) *Biochim. Biophys. Acta 602*, 131−143.
37. Schilling, W. P., and Lindenmayer, G. E. (1984) *J. Membr. Biol. 79*, 163−173.
38. Li, Z., Nicoll, D. A., Collins, A., Hilgemann, D. W., Filoteo, A. G., Penniston, J., Tomich, J. M., and Philipson, K. D. (1991) *J. Biol. Chem. 266*, 1014−1020.
39. Ambesi, A., Van Alstyne, E. L., Bagwell, E. E., and Lindenmayer, G. E. (1991) *Ann. N.Y. Acad. Sci. 639*, 245−247.
40. Cheon, J., and Reeves, J. P. (1988) *J. Biol. Chem. 263*, 2309−2315.
41. Aurora, T. S., Li, W., Cummins, H. Z., and Haines, T. H. (1985) *Biochim. Biophys. Acta 820*, 250−258.
42. Li, W., and Haines, T. H. (1986) *Biochemistry 25*, 7477−7483.
43. Lauger, P. (1987) *J. Membr. Biol. 99*, 1−11.
44. Lauger, P. (1991) in *Electrogenic Ion Pumps*, pp 3−135, Sinauer, Sunderland, MA.
45. Porzig, H., Li, Z., Nicoll, D. A., and Philipson, K. D. (1993) *Am. J. Physiol. 265*, C748−C758.
46. Boerth, S. R., Coetzee, W. A., and Artman, M. (1996) *Ann. N.Y. Acad. Sci. 779*, 536−538.
47. Cannel, M. B., Grantham, C. J., Main, M. J., and Evans, A. M. (1996) *Ann. N.Y. Acad. Sci. 779*, 443−450.
48. Harrison, S. M., and Bers, D. M. (1987) *Biochim. Biophys. Acta 925*, 133−143.
49. Naraghi, M. (1997) *Cell Calcium 22*, 255−268.
50. Doering, A. E., and Lederer, W. J. (1993) *J. Physiol. 466*, 481−499.
51. DiPolo, R., and Beauge, L. (1991) *Ann. N.Y. Acad. Sci. 639*, 100−111.

BI981429U